Three-Dimensional Single Molecule Rotational Diffusion in Glassy State Polymer Films

Andrew P. Bartko, Kewei Xu, and Robert M. Dickson*

School of Chemistry and Biochemistry, Georgia Institute of Technology, Atlanta, Georgia 30332-0400
(Received 8 July 2001; published 24 June 2002)

Measuring three-dimensional orientational motions of many individual molecules within glassy state poly(methyl methacrylate) has enabled nanoscopic probing of bulk-obscured polymer dynamics. Complementing bulk studies, the measured distributions of nanoscale barriers to rotational motion afforded by our single molecule orientational methods directly probe the spatial heterogeneity and nanoscopic α-relaxation dynamics deep within the glassy state.

Coupled with theoretical models of dynamics [1], many bulk [2–6] and single molecule methods [7,8] have been utilized to measure heterogeneous dynamics of glassy state polymers. While much progress has been made, the truly nanoscale intermolecular interactions giving rise to bulk heterogeneity have remained out of reach. Because NMR experiments must probe $\sim 10\ \mu m^3$ regions to obtain sufficient signals, and optical experiments are limited to $\sim 0.1\ \mu m^3$, bulk methods are often too coarse a ruler to measure nanoscale heterogeneity. While average heterogeneous dynamics and length scales (~ 2–3 nm) can be probed [3], bulk methods cannot follow the dynamics of individual heterogeneous sites. Many authors have effectively increased the characteristic length scale of the dynamic heterogeneities by studying translational and rotational diffusion close to the glass transition temperature (T_g) [2–5]. While this is a rich range for studying dynamic heterogeneity, the physical and chemical interactions near T_g differ from those at much more material relevant conditions far below T_g where dynamics are very slow. In both temperature ranges, however, the extreme environmental sensitivity afforded by single molecule studies [9–12] is well suited to probing nanoenvironmental dynamic heterogeneities.

Single molecule orientational microscopy [11,13,14] enables the unobscured dynamics of many individual probes and their unique nanoenvironments to be directly followed, yielding clear information on uncorrelated, out-of-phase motions. Single molecule fluorescence anisotropy studies usually rely on measuring the degree and orientation of linear polarization resulting from the projection of the emission dipole orientation onto a two-dimensional plane. Unless properly accounted for [11,13,15], this results in large uncertainties in out-of-plane angles, especially in the presence of fluorescence intermittency [12]. Bulk measurements are also limited in measuring out-of-plane orientations but additionally lack local environmental sensitivity due to averaging over a broad distribution of environment-influenced uncorrelated motions [16]. Thus, small, fast, uncorrelated motions about an average distribution of molecular orientations are not observable in bulk and likely contribute to the translational-rotational

"paradox" near T_g, in which ensemble-measured translation appears to be orders of magnitude faster than observed rotational motion [4,17].

By employing novel 3D orientational single molecule microscopy methods [11,13], we are able to observe and characterize the spatially heterogeneous room temperature dynamics present in poly(methyl methacrylate) (PMMA) films. Determined by analyzing the spatial distribution of single $DiIC_{18}$ [18] molecule fluorescence when imaged with a CCD camera [11,13], 3D orientational trajectories uniquely enable characterization of nanoscale polymer dynamics. In order to observe molecules of all orientational mobilities with greatly reduced photobleaching, the glass substrate forms the lower window of a microscope-mounted vacuum chamber which is evacuated to $\sim 10^{-5}$ torr. Under these conditions, tens of molecules within a 50 μm^2 field of view are simultaneously imaged for many minutes with 300 msec time resolution with a signal-to-noise ratio of >15 at 5 kW/cm^2 excitation intensity. Utilizing models of single dipoles imaged under high numerical aperture conditions, fits to emission patterns enable single molecule orientations to be followed in time with an accuracy of $\sim 2°$ in θ and ϕ [13]. The total collected intensity for a spatially isolated molecule yields the magnitude of the vector defining orientation and unambiguously indicates the time-dependent intensity $I(t)$, fully separating blinking [12] from molecular orientation.

Independent of intensity (over a 0.5–5 kW/cm^2 range), orientational trajectories are compiled by fitting each emission pattern as a function of time, thereby yielding dipolar orientational trajectories $\mu(\theta, \phi, t)$. Boundary conditions are imposed on the fits such that orientational changes reflect the smallest net angular change without being obscured by degenerate values corresponding to $(\theta, \phi) \rightarrow (-\theta, \phi \pm \pi)$. Individual molecule orientational dynamics are characterized through autocorrelation of the dot product of the intensity-normalized initial dipole orientation, $\mu(\theta, \phi, t_0)$ (or μ_0), with that, μ_τ, at all subsequent discrete time steps: $\langle \mu_0 \cdot \mu_\tau \rangle$. This "memory function" calculates the overlap of the dipole with its original position as a function of observational delay (τ), thereby providing a full description of the rotational dynamics and is

independent of degenerate θ, ϕ pairs, only relying on the angle between the two vectors for each time, τ.

Even at fast moving individual sites, the restricted mobility within polymers results in a significant overlap of the dipole with its initial orientation throughout the observation time. These small, uncorrelated, but significant fast motions are very important in understanding the dynamics in glassy materials, but average out in ensemble measurements [17]. Such fast motions about a slowly evolving average position result in the autocorrelation analysis typically being dominated by the slow processes that are readily measured in bulk studies. The complete knowledge of θ and ϕ throughout the observation times afforded by our single molecule methods, however, yields the time-dependent dynamics and the time-averaged orientational mean. This 3D single molecule mean dipole orientation can be subtracted from each dipole orientation at each time to produce single molecule rotational autocorrelation functions, $P(\tau) = \langle (\mu_\tau - \hat{\mu}) \cdot (\mu_0 - \hat{\mu})/(\mu_0 - \hat{\mu})^2 \rangle$, that emphasize the uncorrelated fast rotational motions characterizing individual sites.

Figure 1 illustrates the different types of observed single molecule rotational motion in room temperature PMMA with corresponding autocorrelation functions. Limiting the range of observable rotational diffusion, twice the sampling interval (Nyquist frequency) and total observation time serve as the lower and upper bounds of the analyzed correlations. Ranges of orientational motion among molecules vary drastically both in magnitudes as well as in rates of orientational change (Fig. 1). While all analyzed molecules can be classified as either mobile or immobile, all molecular trajectories exhibited very different dynamics with wide-ranging characteristic time scales. These orientational dynamics are indicative of the range of polymer heterogeneity on the nanometer scale. Represented by the orientational trajectory and autocorrelation of molecule (a) in Fig. 1, many probe molecules remained locked in one preferred orientation. A smaller portion of the population was found to exhibit greater mobility with wide-ranging dynamics that sampled many orientations (Figs. 1b and 1c). This mobile molecule population is further separated into two subsets: (i) molecules exhibiting fast rotation among multiple preferred orientations about an average position (Fig. 1b) and (ii) molecules that occasionally reoriented, changing between a few discrete, largely immobile preferred orientations (Fig. 1c).

Probe molecules demonstrating only one preferred orientation (Fig. 1a) did not display interesting rotational dynamics. In the rare cases where many orientations were present, oscillatory motion about the mean could clearly be seen in the correlation functions (Fig. 1b). In the intermediate cases, where the orientation changed between preferred, largely immobile directions, autocorrelation analysis still revealed oscillations (Fig. 1c) that arise from a low frequency hopping between fewer discrete molecular orientations. Each rotational autocorrelation
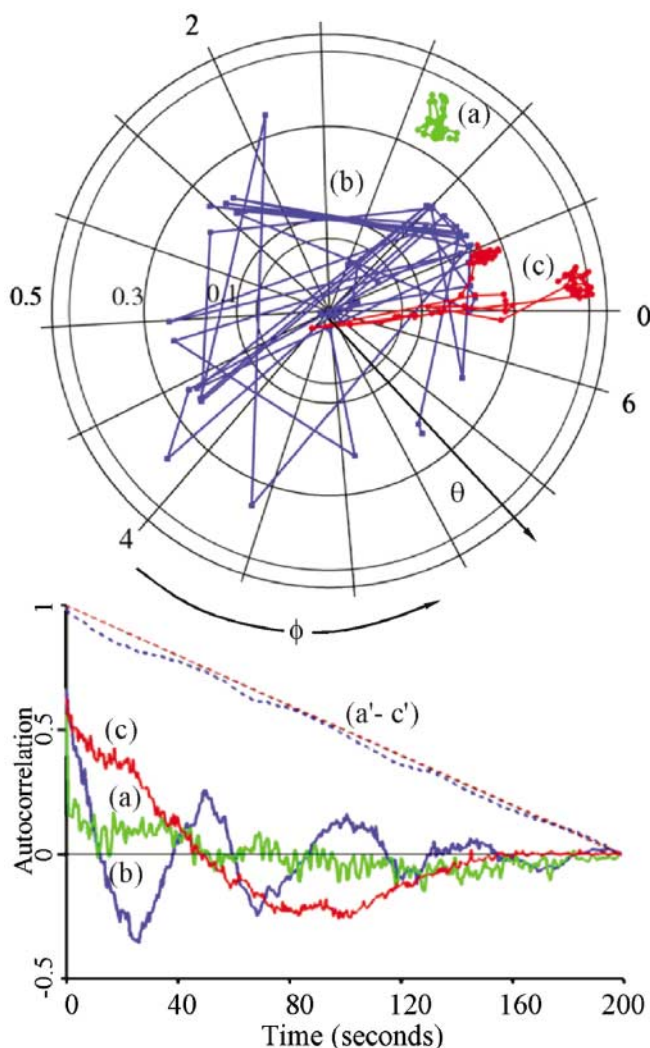

FIG. 1 (color). (top) Three representative single molecule orientational trajectories in PMMA films [(a)−(c), distinguished by line color] are plotted with radial axis θ and angular axis ϕ, in radians. Trajectories are plotted with 75 of several hundred time steps shown for presentation clarity. (bottom) The autocorrelations corresponding to each molecular trajectory [top, (a)−(c)], both with [bottom, (a)−(c)] and without [bottom, (a'-c')] the single molecule mean orientation subtracted. Autocorrelation of molecular motion [bottom, (a'-c')] is dominated by data mismatch at long times indicating strong dipole overlap throughout the observation time. Knowledge of true molecular orientation at all times enables mean subtraction in the autocorrelations [bottom, (a)−(c)], thereby emphasizing the fast, uncorrelated single molecule motions.

is fit to an oscillating exponential decay (Fig. 2a). Free motion within constrained volumes without any preferred stable orientations do not give such oscillations in the orientational autocorrelations. Rotational mobility within the polymer matrix indicated by the exponential decay of the autocorrelation function enables a characteristic decay time, τ, to be extracted. Because the molecule is rotationally restricted, the autocorrelation decay can be loosely related to a pseudorotational diffusion constant
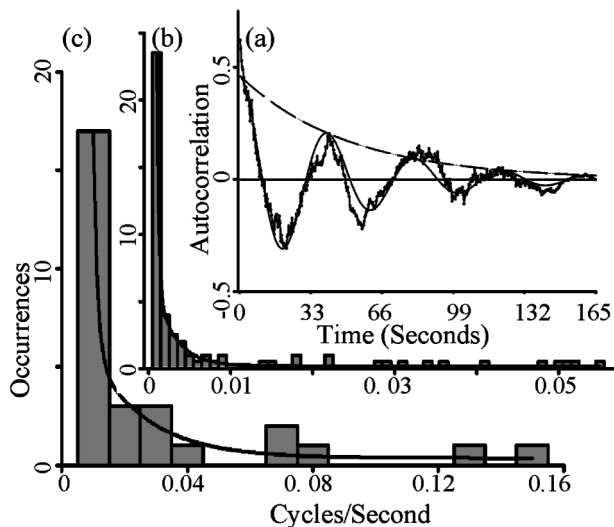
FIG. 2. (a) Oscillating exponential decay fit of a mean-subtracted single molecule rotational autocorrelation. This enables extraction of pseudorotational diffusion constants and reorientation frequencies for each molecule about its average dipole orientation. (b) Histogram of exponential decay constants from 135 molecular rotational autocorrelations observed within $3 \times 10^4 M_n$ PMMA films. (c) Histograms of the rotationally mobile subpopulation (28%) reorientation rates obtained from fits to autocorrelation oscillations. Having the same units, histograms (b) and (c) are overplotted with the best double exponential fits, the poor fit of which at high rates indicates a vast range of heterogeneous environments within the film 80 °C below T_g.

that indicates the time scale for losing memory of the initial dipole orientation via random collisional interactions. However, small hops between preferred orientations in restrictive glassy polymer matrices are observed and result in oscillations of the autocorrelation functions. In agreement with bulk experiments [5,17,19], molecules in such less restrictive sites simultaneously exhibit both increased rotational motion and photochemical degradation.

Room temperature conditions enable a vast range of thermally activated dynamics to occur within PMMA. Such dynamics are commonly characterized through probe molecule reorientation studies [4,5] and can arise from both probe dynamics within a free volume and through polymer dynamics forcing probe molecule motion. In both cases on the single molecule level, the preferred orientations correspond to local potential energy minima in the polymer landscape. Extracted from oscillation frequencies in the autocorrelations and shown in Fig. 2c, a distribution of reorientational rates is present in PMMA that complements the pseudorotational diffusion constants in Fig. 2b. Because our experiments are limited to room temperature and changing molecular weight is in many respects analogous to changing temperature [20], distributions of single probe molecule mobilities were compiled within three different PMMA molecular weight (M_n) samples. Increased chain length ($M_n = 1$, 3, and 5×10^4) shifts the glass transition temperature to higher temperatures

(356, 372, and 385 K, respectively). Converting autocorrelation oscillations from rates to reorientation times, plots of the natural logarithms of average single molecule times vs inverse reduced temperature (T_g/T) yield a straight line, thereby indicating that these single molecule motions are indeed thermally activated. The distributions of reorientational times extracted from the single molecule autocorrelation decays are therefore relatable to distributions of barrier heights to probe reorientation.

Arrhenius analysis performed on activated glassy state dynamic processes seen in analogous systems [4,21] provides an estimated glassy rate ensemble rotational correlation time distribution that, below T_g, remains constant in shape and breadth but shifts to longer times with decreasing temperatures [21]. Because the range of ensemble mobilities exceeds our observation time window, we reconstructed the ensemble distribution [21] corresponding to the percentage of molecules with mobilities falling within our experimental time window. This process allowed estimation of the ensemble average reorientation times as a function of T_g/T. These ensemble average distributions reconstructed from our single molecule reorientation rates demonstrate the Arrhenius behavior within glassy PMMA and yield an activation energy, E_a, of ~250 kJ/mol. This ensemble E_a is directly related to the observed distributions of single molecule reorientation rates (Fig. 2c), which must result from local barrier height distributions. For comparison, bulk probe molecule rotational mobility measurements in poly(isobutyl methacrylate) ($T_g = 326$ K) have shown sub-T_g activation energies of 200 kJ/mol [4]. Thus, observed autocorrelation function oscillations indicate hopping rates between preferred molecular orientations and indicate energy barriers that must be overcome before orientational motion occurs. Each activation barrier uniquely reports on the probe molecule's local environment.

Ensemble measurements [22] clearly show that temperature dependent PMMA α-relaxation dynamics above T_g follow Williams-Landel-Ferry (WLF) scalings. The WLF model [23] accurately represents the rapidly increasing relaxation times observed upon cooling PMMA toward T_g. Extrapolation of sub-T_g Arrhenius behavior and super-T_g WLF behavior with appropriate temperature dependent scalings intersect at T_g when true polymer dynamics (α relaxations) are being probed in both temperature ranges. Replotting published super-T_g WLF data [22] intersects the sub-T_g Arrhenius plot obtained from our 3D single molecule reorientational barrier height distributions precisely at $T = T_g$ (Fig. 3). This indicates not only that the nanoscale probe molecule dynamics are driven by the polymer motions, but also that our single molecule experiments directly probe the nanoscale dynamics resulting from α relaxations deep within the glassy state. Thus, distributions of local barrier heights extracted from single molecule orientational trajectories enable enhanced understandings of the nanoscale interactions
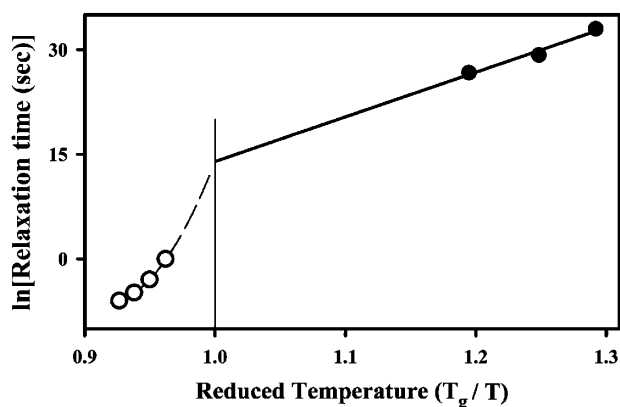
FIG. 3. PMMA single probe molecule reorientation times (filled circles) and bulk α-relaxation processes (open circles, from Ref. [22]), respectively. Three different molecular weight PMMA samples with T_g of 356, 372, and 385 K were used in these studies. Arrhenius and WLF temperature dependent scalings for PMMA, adapted to the T_g/T axis, converge exactly at $T = T_g$. All samples were prepared through spin coating PMMA [24], codissolved with $DiIC_{18}$ as published previously [13].

giving rise to bulk dynamics and are a direct probe of nanoscale heterogeneous polymer dynamics.

———————

*Electronic address: dickson@chemistry.gatech.edu

[1] T. M. Nicholson and G. R. Davies, Macromolecules **30**, 5501 (1997).
[2] K. Schmidt-Rohr *et al.,* Macromolecules **27**, 4733 (1994).
[3] U. Tracht *et al.,* Phys. Rev. Lett. **81**, 2727 (1998).
[4] D. B. Hall, A. Dhinojwala, and J. M. Torkelson, Phys. Rev. Lett. **79**, 103 (1997).
[5] C. Y. Wang and M. D. Ediger, J. Phys. Chem. B **103**, 4177 (1999).
[6] E. V. Russell and N. E. Israeloff, Nature (London) **408**, 695 (2000).
[7] L. A. Deschenes and D. A. Vanden Bout, Science **292**, 255 (2001).
[8] M. A. Bopp *et al.,* Chem. Phys. Lett. **263**, 721 (1996).
[9] W. E. Moerner and L. Kador, Phys. Rev. Lett. **62**, 2535 (1989).
[10] M. Orrit and J. Bernard, Phys. Rev. Lett. **65**, 2716 (1990).
[11] A. P. Bartko and R. M. Dickson, J. Phys. Chem. B **103**, 3053 (1999).
[12] D. A. Vanden Bout *et al.,* Science **277**, 1074 (1997).
[13] A. P. Bartko and R. M. Dickson, J. Phys. Chem. B **103**, 11 237 (1999).
[14] T. Ha *et al.,* Phys. Rev. Lett. **80**, 2093 (1998).
[15] J. T. Fourkas, Opt. Lett. **26**, 211 (2001).
[16] B. J. Berne and R. Pecora, *Dynamic Light Scattering* (John Wiley, Inc., New York, NY, 1976).
[17] M. D. Ediger, Annu. Rev. Phys. Chem. **51**, 99 (2000).
[18] $DiIC_{18}$ (Molecular Probes, Eugene, OR) is 1,1'-dioctade-cyl-3,3,3',3'-tetramethylindocarbocyanine perchlorate.
[19] M. T. Cicerone, F. R. Blackburn, and M. D. Ediger, Macro-molecules **28**, 8224 (1995).
[20] P. J. Flory, *Principles of Polymer Chemistry* (Cornell University Press, Ithaca, NY, 1953).
[21] B. Geil and G. Hinze, Chem. Phys. Lett. **216**, 51 (1993).
[22] G. D. Patterson, P. J. Carroll, and J. R. Stevens, J. Polym. Sci. Polym. Phys. **21**, 613 (1983).
[23] M. L. Williams, R. F. Landel, and J. D. Ferry, J. Am. Chem. Soc. **77**, 3701 (1955).
[24] Number average molecular weight, M_n (1, 3, and 5×10^4), PMMA samples verified through gel permeation chromatography, polystyrene standard in methylene chloride. Glass transition temperatures (356, 372, and 385 K), measured with differential scanning calorimetry 10 °C/min midpoint determination upon a second scan. All PMMA sample tacticities were verified by ^{13}C NMR indicating ~60% syndiotactic.